ELSEVIER

Diamond and Related Materials 11 (2002) 1227–1233

DIAMOND AND RELATED MATERIALS

www.elsevier.com/locate/diamond

Substrate bias effect on amorphous nitrogenated carbon films deposited by filtered arc deposition

Yan-Way Li[a,*], Yew-Bin Shue[a], Chia-Fu Chen[a], Teng-Chien Yu[b], Jack Jyh-Kau Chang[b]

[a]*Institute of Materials Science and Engineering, National Chiao Tung University, Hsinchu 30049, Taiwan, ROC*
[b]*Trace Storage Technology Corporation, Science-Based Industrial Park, Hsinchu, Taiwan, ROC*

Abstract

The effect of substrate bias and nitrogen incorporation on the structure and hardness properties of amorphous carbon (a-C) films is characterized in terms of its composition, sp^3 bonding fraction, and Raman spectra. The films' properties were analyzed using Raman spectroscopy, Auger electron spectroscopy (AES), and nanoindentation system (NIS). Experimental results indicate that a-C films were found to possess the highest hardness when deposited at a substrate bias ranging from -50 to -100 V. In addition, the hardness values do not correlate well with the Raman $I(D)/I(G)$ ratio. The hardness of films increases with their sp^3 bonds fraction. Furthermore, nitrogen content increases with increasing substrate bias on amorphous nitrogenated carbon (a-C:N) films, and influences the growth of small graphitic crystallines.

Keywords: Filtered arc deposition; Amorphous-carbon; Nitrogen; Bias; Hardnesss

1. Introduction

Sputtered amorphous carbon films have been extensively used for the overcoats of magnetic thin film recording disks for the last 20 years [1]. These films have the properties of high wear resistance and chemical inertness, which are the critical requirements of a good overcoat. The thickness of the sputtered carbon films was initially approximately 25 nm, and remained there for a few years until hydrogen and then nitrogen found their ways into the argon sputtering processes. Amorphous hydrogenated carbon (a-C:H) films have comparatively higher hardness, enabling thinner overcoats to be used without compromising the performance and reliability of the hard disk [2,3]. Besides the above research, many results related to the microstructure and tribological performance investigation of nitrogenated carbon (a-C:N) films also have been reported [4,5]. These coatings have to be thin ($\approx$5–20 nm) to minimize the separation between the head and the disk surfaces and thus minimize the loss of read-back signal amplitude. Reduced flying height in modern magnetic storage devices increases the probability of occasional contact between high asperities on the magnetic medium and head surfaces, placing more stringent requirements on the tribological properties of the protective coatings. Tribological properties of amorphous carbon (a-C) vary considerably with the sp^3 to sp^2 bonded carbon ratio, which is dependent on the element composition of the precursor materials and plasma activation processes. A previous study suggested that the deposition of coatings with higher fractions of sp^3 bonded carbon requires the depositing species to have kinetic energies of approximately 80 eV or higher [6]. Generally, a higher fraction of the sp^3 bonded carbon atoms in an amorphous network increases the hardness [7]. Efforts are underway to develop alternative technology for depositing the highest fraction of sp^3 bonded carbon films. The average kinetic energy of the depositing species is known to be very high for the cathodic arc deposition process compared to the other deposition techniques [8]. Consequently, researchers were motivated to develop a new process to produce hydrogen-free, tetrahedral bonding dominated a-C films through filtered arc deposition (FAD).

*Corresponding author.

0925-9635/02/$ - see front matter
PII: S0925-9635(01)00624-0

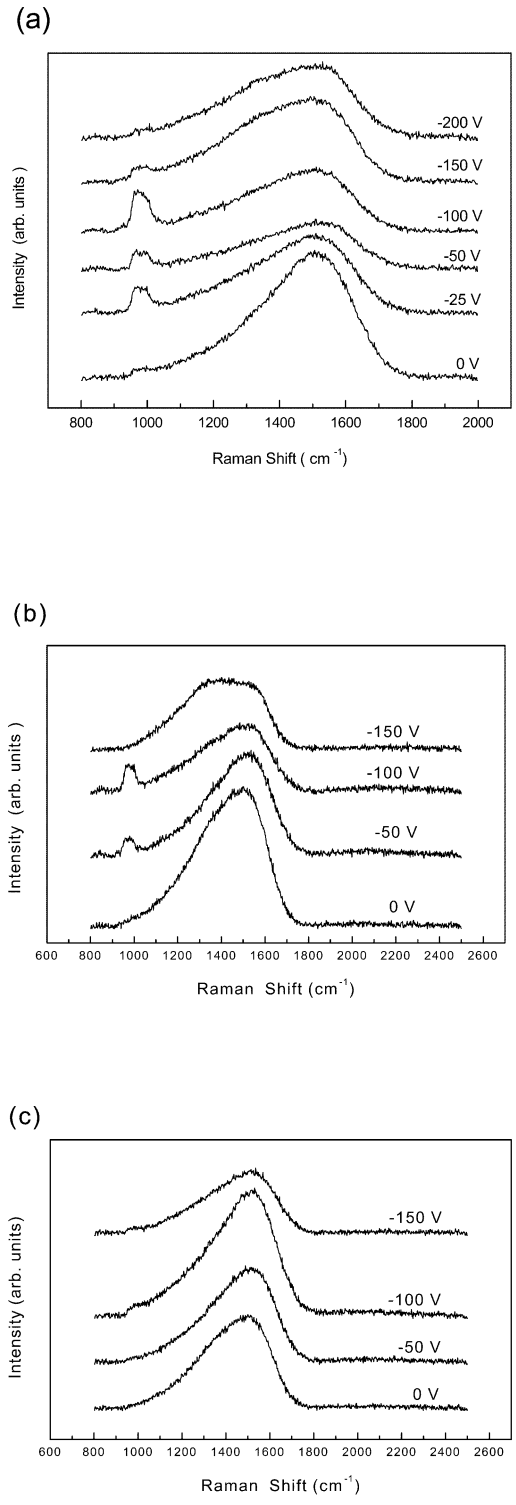

Fig. 1. Raman shift of a-C:N films for various substrate biases and nitrogen gas flow rates, (a) 0 sccm, (b) 2 sccm, and (c) 10 sccm.

Filtered arc deposition is an emerging technology for depositing amorphous hard carbon films [9–11], and has the advantages of a high deposition rate and large area deposition. A magnetic duct filter of the arc plasma removes the neutrals and macro-particles that are produced at the cathode spots along with the plasma, and the cathodic arc can generate highly ionized plasma (30–100%) thus guaranteeing a good diamond-like film quality at low temperatures [12]. Furthermore, the FAD process enables the deposition of ultra-thin amorphous hard carbon films with high sp^3 content, high hardness, chemical inertness, and low friction coefficient. These properties make the FAD process of great interest for head/disk interface application, particularly contact recording. This work aims to investigate the effect of substrate bias and nitrogen incorporation on the bonding configuration and hardness of a-C films deposited using FAD with micro-Raman spectroscopy and nanoindentation system, respectively.

2. Experimental

A FAD apparatus was used to prepare a-C films, as detailed in the previous paper [13,14]. The substrates

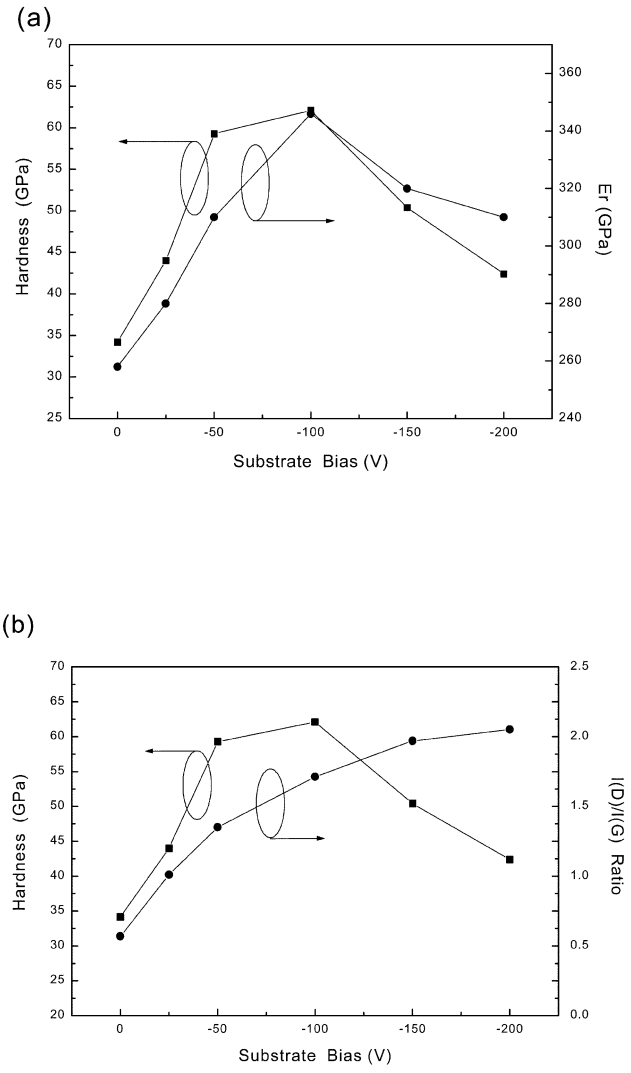

Fig. 2. (a) Hardness and Young's modulus, (b) hardness and Raman $I(D)/I(G)$ ratio of a-C films as a function of substrate bias.

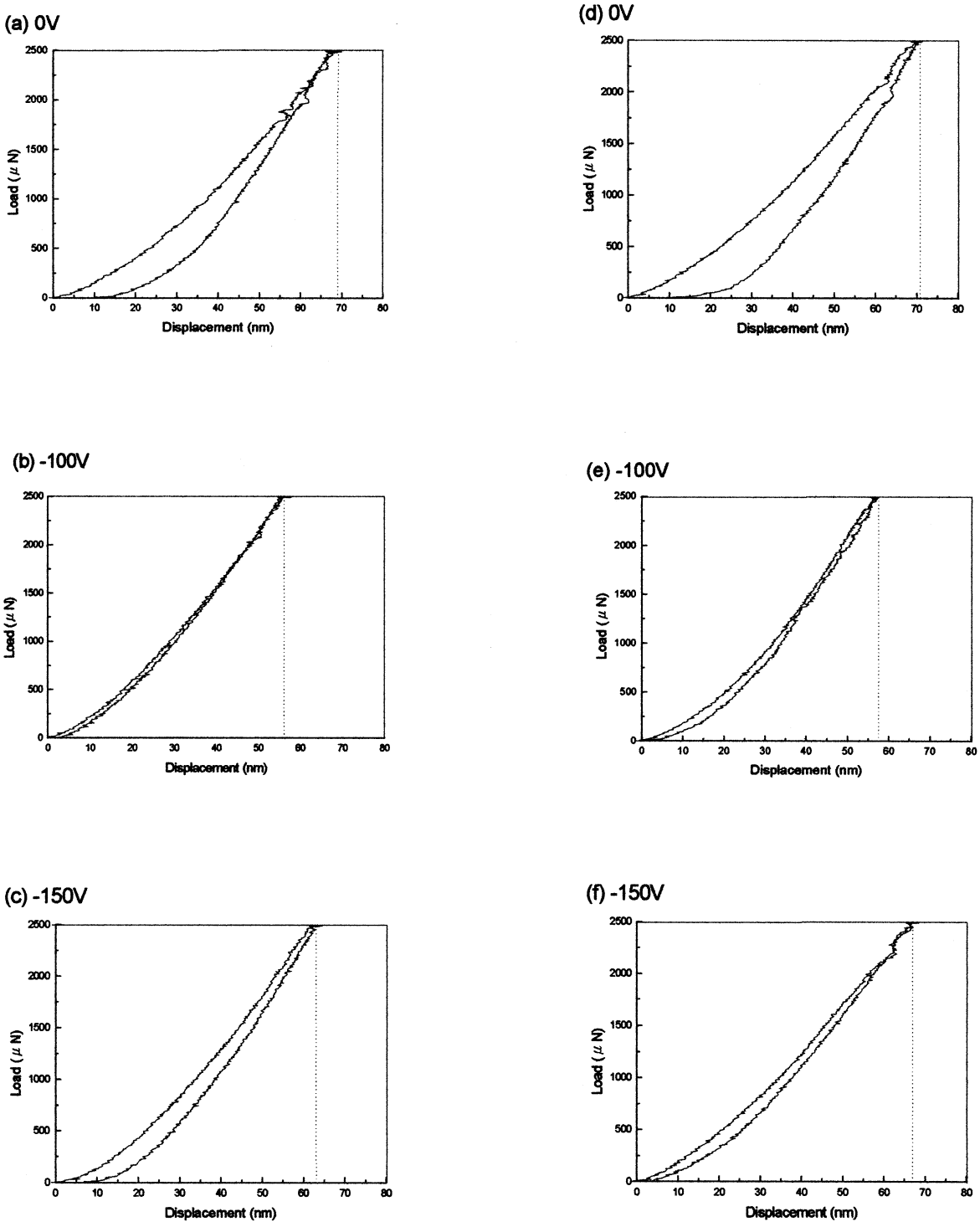

Fig. 3. Loading–displacement plots of nanoindentation, at a 2500 μN peak indentation load, for a-C:N films deposited by FAD with various biases at different nitrogen gas flow rate, (a–c) with 0 sccm, and (d–f) with 2 sccm.

used were (100) p-type silicon wafer with resistivity of ~15–25 Ω cm. The amorphous carbon films under investigation were prepared on substrates at bias voltages ranging from 0 to −200 V. The ion energy is controlled by biasing the substrate and has a relatively narrow energy distribution. Since the filtered beam is nearly 100% ionized, the energy of the carbon ions reaching the substrate can be adjusted by applying a voltage to the substrate holder. The ion current density at the substrate ranges between 10 and 30 mA/cm^2. A high purity graphite (99.9995%) cathode with particle size of 1 μm, was clamped to the water cooled copper

hearth. High purity (99.99%) Ar and N_2 were introduced separately into the deposition system using mass flow controllers. The FAD chamber was evacuated to a base pressure below 5×10^{-6} Torr. The substrates were mounted on a holder, which was negatively dc-biased with respect to the chamber. No extra heating or cooling was applied to the substrate during deposition, but the substrate temperature rises with increasing substrate bias voltage.

Micro-Raman spectroscopy and AES were used to analyze the microstructure and chemical composition, respectively. The mechanical properties were measured using the nanoindentation system, while the microstructure and quality of the amorphous carbon films were determined using Renishaw micro-Raman spectroscopy system 1000. Raman measurements were performed at 514.5 nm at 1 cm^{-1} resolution, and integration took 1 min at 30 mW Ar ion laser power. Raman spectroscopy is a useful non-destructive tool for analyzing carbon films owing to its ability to distinguish different bonding types and domain sizes, and its sensitivity to internal stresses. The Raman peak shift, full width at half maximum (FWHM), intensity, and polarization are the parameters that provide information on film structure. The Auger system used here was a Physical Electronics, model 670 PHI Xi scanning Auger microprobe. The spectra were recorded in the derivative mode using a beam of 5 keV, 0.16 μA electrons. The microhardness of the deposited films was measured using a commercially available nanoindentor (NANO Instruments) with a diamond tip, with an average rate of loading of 100 mN/s, tool nominate depth of 100 nm, the accuracy of monitoring displacement and loading was 2 nm and 2 mN, respectively. Nanoindenter (Hysitron Inc., TriboScopeTM) was employed herein for measuring hardness and AFM (Digital Inc., DimensionTM3000) was used to obtain indentation information.

3. Results and discussion

3.1. Substrate bias effect on a-C films

The Raman spectra of a-C films deposited at various substrate biases are illustrated in Fig. 1a. The Raman spectra of as-deposited a-C films all appear to have a broad asymmetrical shape ranging from 1000 to 1800 cm^{-1} centered at approximately 1530 cm^{-1}. To analyze the spectra quantitatively, the Raman spectra were fitted into two Gaussian peaks using Peakfit [15]. The Raman parameters obtained include the intensity ratio $I(D)/I(G)$, G peak position, and G peak FWHM. The $I(D)/I(G)$ ratio (as shown in Fig. 2b) and wave number of the G peak position increase with increasing substrate bias, while the wave number of G peak FWHM decreases. Similar results regarding the increase in wave number for the G peak position were also reported by Zhang et al. [19] for the a-C films deposited using the magnetron sputtering technique. According to them, this could be because a higher bias voltage leads to an increase in substrate temperature and thus causing graphitic particles to be introduced to the amorphous carbon matrix.

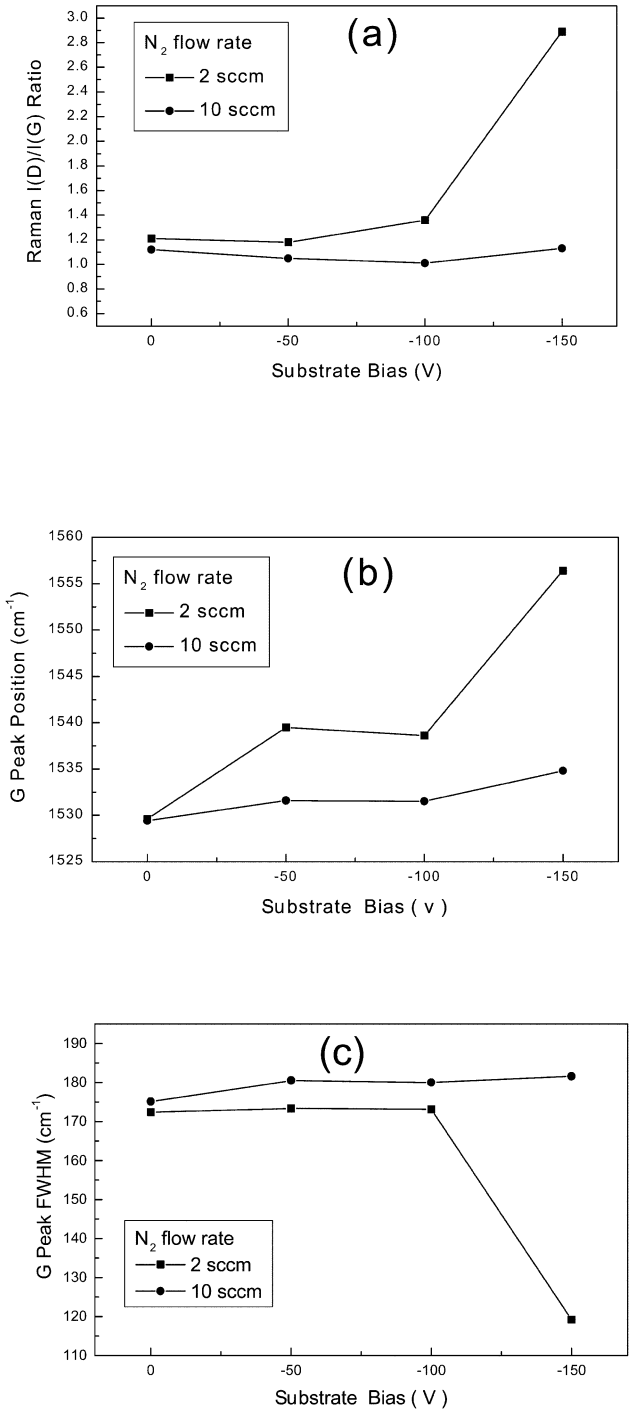

Fig. 4. (a) Raman $I(D)/I(G)$ ratio, (b) Raman G peak position, (c) Raman G peak FWHM of a-C:N as a function of substrate bias.

For the FAD process, the lowest $I(D)/I(G)$ ratios are generally reported for the bias voltage range of -50 to

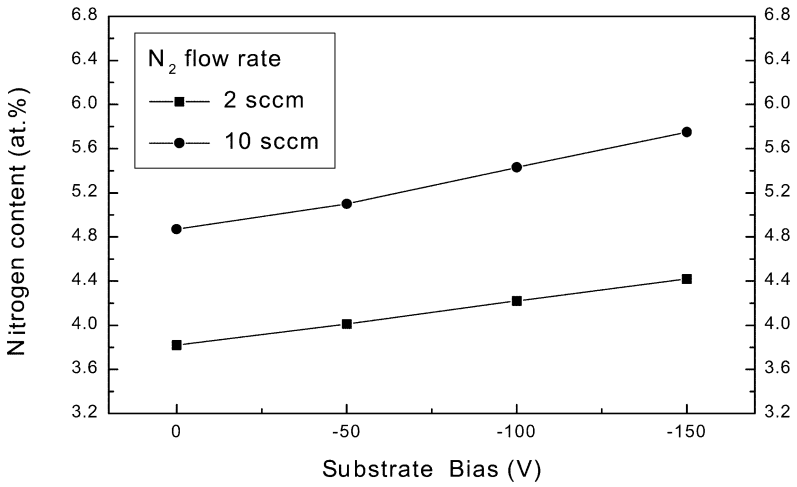

Fig. 5. Nitrogen content in the a-C:N films as a function of substrate bias at nitrogen gas flow rate 2 and 10 sccm, analyzed by AES.

−120 V [16–18]. However, in the present case, the lower $I(D)/I(G)$ intensity rations are seen for the films deposited at 0 V. This is more desirable, since the lower $I(D)/I(G)$ ratio indicates the higher sp^3 content and thus has a more diamond-like character [19].

In fact, another observation that should be noted in Fig. 1a is the existence of a peak at $\sim 965\ cm^{-1}$, indicating the point where the second order phonon scatters from the silicon substrate. The appearance of this peak is an indicator of the transparency of the film near the laser wavelength of 514 nm [20], and indicates that the films become more transparent when the substrate bias is between −25 and −100 V. Since the high transparency results from the film's high sp^3 content, the high transparency of the film deposited at −100 V results from the high fraction of carbon atoms with tetrahedral coordination, which indicated the film's high sp^3 bonding content. According to the two phase or clustered model proposed by Robertson [21,22], the structure of a-C films with various substrate biases can be interpreted as follows: the substrate temperature will increase with increasing substrate bias. The higher plasma energy may be due to the graphitization or partial graphitization of microscopic regions in the amorphous matrix. As the substrate bias increases, the graphitic clusters grow in size and/or number, contribute to the D peak, and increase the $I(D)/I(G)$ ratio (Fig. 1a). However, the bonding in the amorphous matrix should have a higher fraction of carbon atoms with tetrahedral coordination at the proper substrate bias (−50 to −100 V). This can be verified by the existence of a peak at approximately $965\ cm^{-1}$ in the Raman spectra illustrated in Fig. 1.

Hardness is the key parameter of technologically relevant diamond-like carbons. The mechanical properties of the a-C films were investigated using the nanoindentation technique, which is measured by indentation and is the pressure over the permanently indented area at a given applied load. The nanoindentation technique reveals a strong dependence on the film microstructure, composition, and deposition parameters. The hardness and Young's modulus can be calculated according to the load–displacement plots of a-C films. The hardness and Young's modulus are plotted against substrate bias and displayed in Fig. 2. It showed the hardness increases to maximum value of approximately 62 GPa at the bias voltage of −100 V and then decreases thereafter. The Young's modulus measurement has the same trend with hardness in the bias rang and has a maximum value of 346 GPa at −100 V. The hardness is approximately one-sixth of the Young's modulus herein, conforming with the prediction of Robertson [21]. Fig. 2b indicates that film hardness does not correlate strongly with the Raman $I(D)/I(G)$ Ratio. The high hardness is attributed to the high fraction of sp^3 content in the amorphous carbon matrix, and the hardness of the corresponding films is not related to the sp^2 bonding disorder. Fig. 3 illustrates the loading–displacement plots of the corresponding films. Bigger indentation and deeper depth clearly correspond to softer films, while smaller indentation and depth correspond to harder films.

3.2. Substrate bias effect on a-C:N films

a-C:N films were deposited for various substrate biases at a low (2 sccm) and high nitrogen flow rates (10 sccm) respectively. Fig. 1b,c displays that the Raman spectra of the a-C:N films with a low nitrogen flow rate are similar to those of amorphous carbon, as shown in Fig. 1a, but the spectra at high nitrogen flow rate, shown in Fig. 1c, is slightly different from that in Fig. 1b. The peak at $\sim 965\ cm^{-1}$ disappears, indicating that a-C:N films under high nitrogen gas flow rate have weak transparency near the laser wavelength of 514 nm,

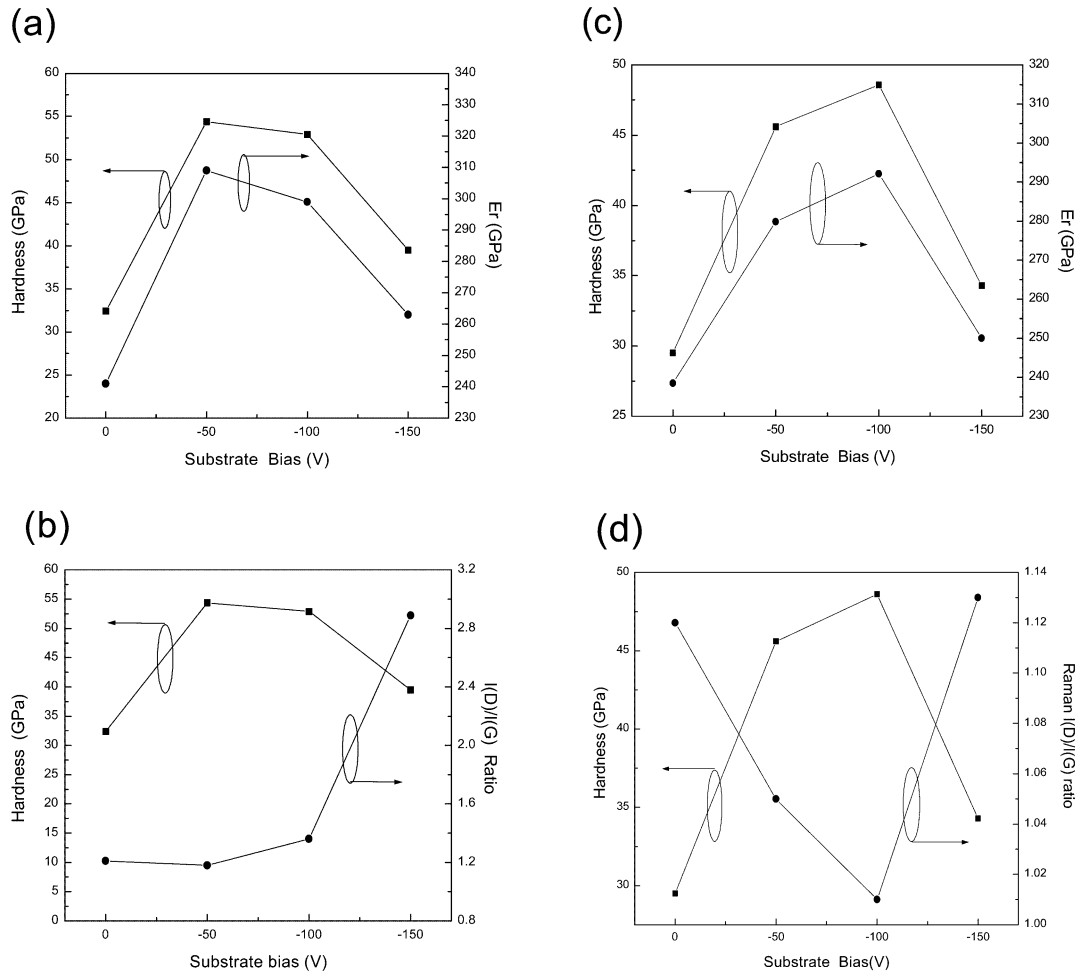

Fig. 6. Hardness, Young's modulus and Raman $I(D)/I(G)$ ratio of a-C:N films as a function of substrate bias at different nitrogen gas flow rate, (a,b) with 2 sccm, (c,d) with 10 sccm.

and also indicates that the films have higher sp^2 bonding. The Raman parameters, including the intensity ratio $I(D)/I(G)$, G peak position and G peak FWHM, were presented in Fig. 4, which shows that the Raman parameters did not change drastically at high nitrogen flow rate, when the substrate bias fell below -150 V. This phenomenon ascribes that the substrate bias is not obviously connected with the graphitic crystallizing on the films deposited at high nitrogen flow rates. The spectra present the same result on the films deposited at a low nitrogen flow rate with substrate biases exceeding -100 V, but the $I(D)/I(G)$ ratio and the G peak position increases abruptly, yet G peak FWHM decreases when the substrate bias is between -100 and -150 V. This behavior probably indicates a significant amount of small graphitic crystalline grows when the substrate is biased between -100 and -150 V, while the ratio of sp^2-distorted to undistorted bonds increases. Fig. 5 shows the Auger compositional analysis of the corresponding a-C:N films. Auger microprobe measurements of the depth profile of a-C:N films revealed a uniform distribution of nitrogen throughout the film. According to the Auger surface compositional analysis of the a-C:N films with a high rate of nitrogen gas flow, the greater incorporation of nitrogen in the high substrate bias may result from the C≡N bonding [23,24].

The hardness, Young's modulus, and $I(D)/I(G)$ ratio of the a-C:N films as a function of substrate bias were plotted in Fig. 6. The hardness and Young's Modulus also exhibit the same trend as the a-C films with increasing negative substrate bias. According to the above discussion, higher hardness at the substrate bias between -50 and -100 V should be attributed to the high sp^3 content. In addition to the low sp^3 content, the low hardness at 0 and -150 V is probably attributed to the C≡N triple bonds. These bonds obstruct the formation of carbon–carbon cross-linking [25], softening the films. The sudden increase of the $I(D)/I(G)$ ratio under low nitrogen gas flow rate, illustrated in Fig. 6b, does not affect the hardness value. Again, it suggests that the graphitic crystallizing will not clearly influence the film hardness. Fig. 6d displayed that the $I(D)/I(G)$ ratio

seems to influence the hardness of a-C:N film as much as does a high rate of nitrogen gas flow. Notably, the $I(D)/I(G)$ ratio fluctuates within a small range, and it is impossible to obtain a good correlation between film hardness and the $I(D)/I(G)$ ratio. Fig. 3d–f illustrates the loading–unloading curves of a-C:N films given a nitrogen flow rate of 2 sccm.

Acknowledgments

The authors would like to thank the National Science Council of the Republic of China for financially supporting this research under contract no. NSC89-2216-E-009-042.

References

[1] F.K. King, IEEE Trans. Magn. 17 (4) (1981) 1376.
[2] Z. Jiang, C.-J. Lu, D.B. Bogy, C.S. Bhatia, T. Miyamoto, IEEE Trans. Magn. 31 (6) (1995) 3015.
[3] M.K. Fung, W.C. Chan, K.H. Lai, I. Bello, C.S. Lee, N.B. Wong, S.T. Lee, J. Non-Cryst. Solids 254 (1999) 167.
[4] N. Laidani, A. Miotello, J. Perrière, Appl. Surf. Sci. 99 (1996) 273.
[5] G. Wang, J.M. Silversten, J.H. Judy, G.L. Chen, J. Appl. Phys. 339 (1999) 74.
[6] D.R. McKenzie, D. Muller, B.A. Pailthorpe, Phys. Rev. Lett. 67 (6) (1991) 773.
[7] J.J. Cuomo, D.L. Pappas, J. Bruley, J.P. Doyle, K.L. Saenger, J. Appl. Phys. 70 (3) (1991) 1706.
[8] B.K. Gupta, B. Bhushan, Wear 190 (1995) 110.
[9] D.R. Mckenzie, D. Muller, B.A. Pailthorpe, Z.H. Wang, E. Kravtchinskaia, D. Segal, P.B. Lukins, P.J. Matrin, G. Amaratunga, P.H. Gaskell, A. Saeed, Diamond Relat. Mater. 1 (1991) 51.
[10] I.I. Aksenov, V.E. Strel'nitskii, Surf. Coat. Technol. 47 (1991) 98.
[11] S. Anders, A. Anders, I.G. Brown, B. Wei, K. Komvopoulos, J.W. Ager, K.M. Yu, Surf. Coat. Technol. 68/69 (1994) 388.
[12] S. Anders, A. Anders, I.G. Brown, J. Appl. Phys. 74 (1993) 4239.
[13] Y.-W. Li, C.-F. Chen, Y.-J. Tseng, Jan. J. Appl. Phys. 40 (2A) (2001) 777.
[14] J.P. Zhao, X. Wang, Z.Y. Chen, S.Q. Yang, T.S. Shi, X.H. Liu, S.C. Zou, Nucl. Instrum. Methods B 127/128 (1997) 1.
[15] M.A. Tamor, W.C. Vasell, J. Appl. Phys. 76 (1994) 3823.
[16] M. Yoshikawa, G. Katagiri, H. Ishida, A. Ishitani, J. Appl. Phys. 64 (1988) 6464.
[17] B.K. Tay, X. Shi, H.S. Tan, H.S. Yang, Z. Sun, Surf. Coat. Technol. 105 (1998) 155.
[18] D. Chen, A. Wei, S.P. Wong, S. Reng, J.B. Xu, I.H. Wilson, J. Non-Cryst. Solids 254 (1999) 161.
[19] S. Zhang, X.T. Zeng, H. Xie, P. Hing, Surf. Coat. Technol. 123 (2000) 256.
[20] T.A. Friedman, K.F. McCarty, J.C. Barbour, M.P. Siegal, D.C. Dibble, Appl. Phys. Lett. 68 (1996) 1643.
[21] J. Robertson, Surf. Coat. Technol. 50 (1992) 185.
[22] J. Robertson, Phys. Rev. Lett. 68 (1992) 220.
[23] X.A. Zhao, C.W. Ong, Y.C. Tsang, P.W. Chan, C.L. Choy, Appl. Phys. Lett. 66 (1995) 2652.
[24] Z.J. Zhang, S. Fan, J.L. Huang, C.M. Lieber, J. Electron. Mater. 25 (1996) 57.
[25] F.S. Pool, Y.H. Shing, J. Appl. Phys. 68 (1990) 62.